Rapid Communications

Deterministic approach to skyrmionic dynamics at nonzero temperatures: Pinning sites and racetracks

Josep Castell-Queralt, Leonardo González-Gómez, Nuria Del-Valle, and Carles Navau*
Departament de Física, Universitat Autònoma de Barcelona, 08193 Bellaterra, Barcelona, Catalonia, Spain

(Received 6 February 2020; revised manuscript received 27 March 2020; accepted 30 March 2020; published 16 April 2020)

The discovery of room-temperature skyrmions in some magnetic materials has boosted the investigation of their dynamics in view of future applications. We study the dynamics of skyrmions in the presence of defects or borders using a deterministic (finding and solving a deterministic Fokker-Planck differential equation) while probabilistic (the solution is the probability density for the presence of a skyrmion) approach. The probability that a skyrmion becomes trapped in a pinning center or the probability of the survival of a skyrmion along a racetrack are obtained as a function of temperature. The present work can be relevant in the design of skyrmionic devices where the probability of finding skyrmions at a given position and time is crucial for their feasibility.

DOI: 10.1103/PhysRevB.101.140404

Magnetic skyrmions are whirling magnetic structures that can be found on certain magnetic materials [1]. Their small size and high mobility have promoted them as promising information carriers as well as basic elements in ultradense magnetic memories, logic devices, or computational systems [2–6]. In ferromagnetic ultrathin films, it has been found that skyrmions can be stabilized with the aid of interfacial Dzyaloshinskii-Moriya (iDM) interactions with a heavy-metal substrate [7–10]. The same mechanism allows the formation of skyrmions in multilayers with alternate ferromagnets and heavy metals [11,12]. The experimental discovery of room-temperature skyrmions [13] has boosted the potentiality of skyrmions for applications and, as a result, the study of their current-driving dynamics at nonzero temperatures.

Skyrmionic racetracks were proposed to transport skyrmions using the spin-orbit torque produced by a spin-polarized current fed into a heavy-metal substrate [2,14]. In such systems, defects or granularity result in a threshold current density for the activation of the movement [15–20] and the borders of the track create a confining potential that sets a driving velocity threshold above which the skyrmions would escape [21–24]. At increasing temperature, the stochastic effects on the skyrmions' position [25–27] could compromise their existence when approaching the borders or defects [22,28]. Also, their topological protection is weakened, which can lead to their collapse [22,29–32]. This stochastic motion sets different conditions (or restrictions) on the applicability of racetracks that should be addressed. In particular, some questions arise: What is the probability for the skyrmion to escape from a pinning center? What is the probability for a skyrmion to overcome the racetrack border's confining potential? What is the probability of finding a skyrmion at a given distance from the initial position after a given time?

At temperature $T = 0$ the movement of the skyrmion is not probabilistic [21,23,33,34] and the previous questions do not apply. The inclusion of thermal effects in micromagnetic simulations can be done either by using a stochastic Landau-Lifshitz-Gilbert equation, Landau-Lifshitz-Bloch equation, or by stochastic atomic spin dynamics [35–38]. Thiele's equation [39], originally introduced for magnetic bubble domain motion, with the inclusion of extra stochastic terms [stochastic Thiele's equation (STE)], is also used to study the dynamics of skyrmions [17,25,27,28,40,41]. In this case, it is assumed that the skyrmion maintains its shape during the movement (rigid approximation). Even at room temperature, this assumption can be a valid approximation as shown for Pt/Co/Ir, Pt/CoFeB/MgO, or Pt/Co/Ta multilayers [13,20]. In all these cases, the simulations for a single skyrmion have to be repeated a large number of times and the average quantities evaluated with the corresponding statistical dispersion.

Here, we use a deterministic, while probabilistic, approach for studying the dynamics of skyrmions including temperature. We evaluate the effects of pinning potentials as well as racetrack borders. Instead of solving the STE many times, we solve the corresponding deterministic Fokker-Planck equation [42] (FPE) for the probability density of the presence of a skyrmion as a function of time. The main advantages of this approach are as follows: (i) One needs to solve the FPE only once; (ii) some approximations can be analytically worked out; (iii) FPE is a partial differential equation that can be solved using well-known numerical techniques (even commercial software); and (iv) complex potentials can be included without a significant increase in the computation time.

Some previous works have also used the same deterministic approach for studying the dynamics of rigid skyrmions [26,43] (and vortices [44]). In Ref. [26] the mobility of skyrmions in a periodic potential was evaluated in the stationary limit. Also, in Ref. [43] the steady-state velocity (of antiferromagnetic skyrmions in this case) for the lowest-order traveling wave solutions of the probability density was obtained. In contrast to these works, here we obtain the full time and position dependence of the solution of the FPE for

*Corresponding author: carles.navau@uab.cat

the case in which rigid skyrmions travel in the presence of a pinning site or along a racetrack. From these solutions, all the probabilistic properties of the dynamics can be obtained.

Our starting point is the stochastic Thiele's equation for a rigid skyrmion moving on a magnetic ultrathin film (thickness d, volume V) with background magnetization pointing in the $-\hat{\mathbf{z}}$ direction and located on the $z = 0$ plane. The movement of the skyrmion is described by the position of its center of mass whose time derivative is the velocity of the skyrmion $\mathbf{V}_s$. We consider here that the skyrmion is driven through dampinglike torques produced by spin-polarized currents coming from the spin-Hall effect after feeding an in-plane current $\mathbf{J}_H$ in a heavy-metal substrate [45]. The STE can be written as [46]

$$(\mathbb{G} - M_s\alpha\mathbb{D})\mathbf{V}_s + M_s\mathbb{N}\mathbf{V}_H + \gamma M_s^2(\mathbf{F}_{\text{ext}} + \mathbf{F}_{\text{st}}) = \mathbf{0}, \quad (1)$$

where $\mathbb{G}$ and $\mathbb{D}$ are the gyrocoupling and dissipation matrix, respectively. $\mathbb{N}$ comes from the integration of the spin-transfer torque term in the Landau-Lifshitz-Gilbert equation. They all are 2×2 matrices whose elements are $(u, v = x, y)$ $\mathbb{G}_{uv} = \int_V \mathbf{M}_0 \cdot (\frac{\partial \mathbf{M}_0}{\partial u} \times \frac{\partial \mathbf{M}_0}{\partial v})dV$, $\mathbb{D}_{uv} = \int_V (\frac{\partial \mathbf{M}_0}{\partial u} \cdot \frac{\partial \mathbf{M}_0}{\partial v})dV$, and $\mathbb{N}_{uv} = (1/d)\int_V (\frac{\partial \mathbf{M}_0}{\partial u} \times \mathbf{M}_0)_v\, dV$. $\mathbf{V}_H = -\frac{\mu_B \theta_H}{eM_s}(\mathbf{z} \times \mathbf{J}_H)$, with μ_B the Bohr magneton, θ_H the Hall angle, and e (>0) the charge of the electron. In the present case, considering axisymmetric skyrmions, $\mathbb{G}_{xy} = -\mathbb{G}_{yx} \equiv G$, $\mathbb{D}_{xx} = \mathbb{D}_{yy} \equiv D$, $\mathbb{N}_{xy} = -\mathbb{N}_{yx} \equiv -N$, where $G > 0$, $D > 0$, and $N > 0$. All other elements of the matrices are zero. γ is the gyromagnetic constant ($\gamma = 2.21 \times 10^5$ m A^{-1} s^{-1}), α is the Gilbert damping constant, and M_s the saturation magnetization. The force terms $\mathbf{F}_{\text{ext}}$ and $\mathbf{F}_{\text{st}}$ come, respectively, from the external and stochastic forces.[1] $\mathbf{F}_{\text{st}}$ is considered a white noise with $\langle F_{\text{st},j}\rangle = 0$ and $\langle F_{\text{st},i}\, F_{\text{st},j}\rangle = \frac{2\alpha D k_B T}{\gamma \mu_0 M_s}\delta_{ij}\delta(t - t')$ [25], with $i, j = x, y, z$, μ_0 the vacuum permeability, k_B the Boltzmann constant, δ_{ij} the Kronecker delta, and $\delta(t - t')$ the temporal Dirac's delta.

For a given initial position of the skyrmion, the stochastic nature of Eq. (1) results in different trajectories for each simulated solution. However, the probability density of finding the center of mass of the skyrmion at position $\mathbf{r} = (x, y)$ and time t, $p(\mathbf{r}, t)$, can be directly evaluated from its corresponding FPE (see Supplemental Material for the derivation [47]) that can be written as

$$\frac{\partial}{\partial t}p(\mathbf{r}, t) = -\nabla \cdot [p(\mathbf{r}, t)(\mathbf{V}_{\text{drv}} + \mathbf{V}_{\text{ext}})] + D_d\nabla^2 p(\mathbf{r}, t), \quad (2)$$

where we have used the definitions

$$D_d = \frac{\gamma M_s^3 \alpha D k_B T}{\mu_0(G^2 + D^2\alpha^2 M_s^2)}, \quad (3)$$

$$\mathbf{V}_{\text{drv}} = -(\mathbb{G} - \alpha M_s\mathbb{D})^{-1} M_s\mathbb{N}\mathbf{V}_H, \quad (4)$$

$$\mathbf{V}_{\text{ext}} = -(\mathbb{G} - \alpha M_s\mathbb{D})^{-1}\gamma M_s^2\mathbf{F}_{\text{ext}}. \quad (5)$$

Equation (2) is a convection-diffusion equation. The first term on the right-hand side indicates that the probability density is transported at a velocity $\mathbf{V}_{\text{drv}} + \mathbf{V}_{\text{ext}}$, whereas the second term is a linear, homogeneous, and isotropic diffusion term with constant D_d. Actually, the FPE is also a continuity equation

$$\frac{\partial}{\partial t}p(\mathbf{r}, t) = -\nabla \cdot \mathbf{J}_p(\mathbf{r}, t), \quad (6)$$

where one can define the current of probability density $\mathbf{J}_p(\mathbf{r}, t) = (\mathbf{V}_{\text{drv}} + \mathbf{V}_{\text{ext}})p(\mathbf{r}, t) - D_d\nabla p(\mathbf{r}, t)$.

Equation (2) can be analytically solved in some cases. If one considers a free skyrmion [no driving ($\mathbf{V}_H = \mathbf{0}$), no external forces ($\mathbf{F}_{\text{ext}} = \mathbf{0}$)], whose initial position probability density is described by a Gaussian function centered at the origin of coordinates with a given variance σ^2, $p_0(x, y) = \mathcal{N}(0, \sigma)$, the solution of Eq. (2) is $p(x, y, t) = \mathcal{N}(0, \sqrt{\sigma^2 + 2D_d t})$, which indicates that the initial Gaussian distribution diffuses without translation, maintaining the Gaussian shape, where the variance is a linear function of the time and proportional to the temperature. These results are in complete agreement with Ref. [25] which used a completely different approach (thermal agitation of classical spins on a triangular lattice) to monitor the Brownian motion of skyrmions.

Another interesting analytical solution of the FPE is the stationary ($t \to \infty$) solution of the probability density when a harmonic pinning center is present. In this case, if the pinning center is at the origin, the force felt by the skyrmion can be described by $\mathbf{F}_{\text{ext}} = -k(x\hat{\mathbf{x}} + y\hat{\mathbf{y}})$ (k indicates the restoring coefficient of the force, assumed constant). No driving current is considered. The stationary solution of Eq. (2) is found to be, independently of the initial probability density, $p(x, y, \infty) = \mathcal{N}(0, \sqrt{\frac{M_s k_B T}{\mu_0 D_d k}})$. It is also a Gaussian distribution whose variance increases linearly with temperature and is inversely proportional to k. This indicates that the skyrmion, regardless of the initial position, will go to the pinning site, jiggling around it with a variance that represents a competition between the thermal diffusive effect and the attractive pinning force.

Consider a more realistic case of a skyrmion driven by current density $\mathbf{J}_H$ which finds an attractive pinning center whose force is described by [46]

$$\mathbf{F}_{\text{ext}} = -F_{0p}\frac{\mathbf{r}}{\lambda}\exp\left(-\frac{|\mathbf{r}|^2}{\lambda^2}\right), \quad (7)$$

where λ and F_{0p} control the scope and the strength of the pinning potential, respectively. Although only the position of the center of mass of the skyrmion is evaluated, the rigid model assumes a fixed shape of the skyrmions. However, its radius can change in an order of magnitude from $T = 0$ to room temperature [20,31]. Since λ in Eq. (7) is related to the radius of the skyrmion [21], we set $\lambda = R_s$ and we use the results of Ref. [31] to find its dependence on T (see Supplemental Material for the details [47]). $\lambda(T)$ increases with temperature in a nonlinear way, with a larger slope at larger temperatures. We assume that G and D are independent of temperature (models predict that G is basically independent of the radius and that D depends on the diameter/domain wall width ratio [40,48]; we are thus assuming that the change in temperature maintains this ratio constant).

[1] Strictly, $\mathbf{F}_{\text{ext}}$ and $\mathbf{F}_{\text{st}}$ do not have units of force, but we follow the usual nomenclature.

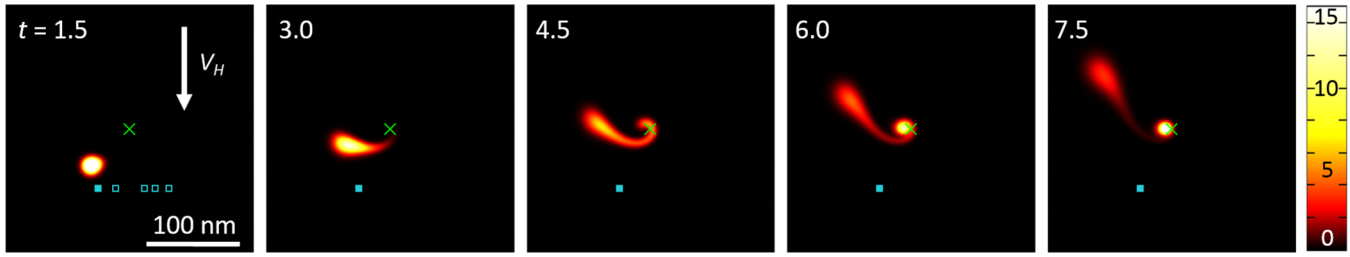

FIG. 1. Snapshots for the probability density $p(\mathbf{r}, t)$ (color bar in units of 10^{-3} nm^{-2}), evaluated at different times, indicated in each figure in ns. The central green cross indicates the position of the pinning center and the solid blue square indicates the initial position. The open blue squares indicate the initial position of the skyrmions considered in Fig. 2. The parameters used in this simulation are $T = 150$ K, $\alpha = 0.3$, $M_s = 580$ kA m^{-1}, $D = G = 4\pi$, $V_H = 277.4$ m s^{-1}, $\lambda(T) = 38.3$ nm, and $F_{0p} = 5.8 \times 10^{-14}$ m^2 A^{-1}. See Supplemental Material for numerical details and video [47].

We want to evaluate the probability that a skyrmion is trapped by this pinning center, as a function of the temperature. The resulting FPE [Eqs. (2)–(5) with Eq. (7)] has to be solved numerically (see Supplemental Material [47] and Ref. [49] for the numerical details). Results do depend on the initial position of the skyrmion. As described in Ref. [46] for $T = 0$, for a given V_H below a threshold velocity, the solution of Thiele's equation yields two differentiated regimes depending on the initial position of the skyrmion: (i) The skyrmion is trapped and (ii) the skyrmion escapes. Actually, there is a saddle point in the $T = 0$ phase portrait of the trajectories that determines if the skyrmion is or is not trapped, depending on from which side of the saddle point the skyrmion is approaching. However, at $T > 0$ these two regimes are not so clearly differentiated. Due to the thermal diffusion, it is possible that a skyrmion that would escape at $T = 0$ does not at $T > 0$. The opposite is also true: A skyrmion that would be trapped at $T = 0$ has some "thermal chance" of escaping. We show in Fig. 1 some snapshots, at different times, of the calculated probability density $p(x, y, t)$ in a region close to a pinning center (indicated as a green cross) for a given initial position (blue solid square) and a given temperature ($T = 150$ K). We observe that some probability density escapes from the pinning center. After a long time the situation stabilizes and the probability of being trapped,

$$P_t = \int_{S_c} p(x', y', \infty) dx'\, dy', \tag{8}$$

can be evaluated. To evaluate P_t, we have considered a calculation window S_c of dimensions much larger than $\lambda(T) \times \lambda(T)$. Note that the persistence of the driving currents makes that the final probability density distribution is not centered on the pinning site but at a nearby position [46,50].

In Fig. 2 we show the calculated P_t as a function of the temperature, for different initial positions. At $T = 0$ the situation is binary: P_t is either one or zero, depending on the initial position. Increasing T, the potential well becomes broader and shallower [due to the $\lambda(T)$ dependence], increasing the probability for those skyrmions that would escape at $T = 0$ (red lines) to fall into the well at relatively low T. At the same time, for those skyrmions that would be trapped at $T = 0$ (blue lines) the probability of trapping decreases when the potential becomes shallower, although the broadening acts as a counteracting effect. Finally, at large T, regardless of the initial position of the skyrmions, the thermal energy overcomes the potential well and P_t goes to zero in all cases. An increase in the F_{0p} factor would shift the temperature at which P_t goes to zero to higher values.

One of the important issues in the skyrmionic roadmap is the transport along racetracks [2]. The feasibility of such systems is based on the survival of skyrmions when they are driven along the racetrack. We now want to evaluate the probability of such a survival. Consider a long racetrack along the x axis, with a width $2W$ in the y axis (the center line of the racetrack is $y = 0$). The force over the skyrmion due to the borders can be modeled as [21]

$$\mathbf{F}_{\text{ext}} = F_{0t}\big[- e^{-\frac{W-y}{\lambda}} + e^{-\frac{W+y}{\lambda}} \big]\hat{\mathbf{y}}. \tag{9}$$

The corresponding FPE [Eqs. (2)–(5) with Eq. (9)] is also solved numerically (see Supplemental Material for numerical details [47]). In Fig. 3 we show the probability density evolving with time for two temperatures [$T = 100$ K in Fig. 3(a), and $T = 300$ K in Fig. 3(b)] at a fixed driving

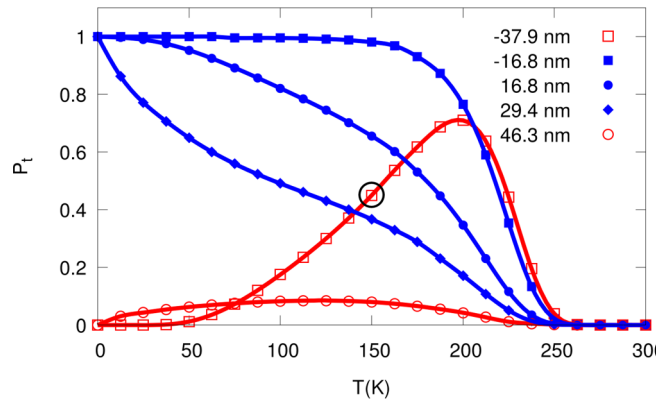

FIG. 2. Probability P_t that a skyrmion is trapped in a Gaussian pinning center when it is driven by currents as a function of the temperature, for different initial positions of the skyrmion, indicated with the x coordinate with respect the green cross in Fig. 1 (the initial positions are shown as open blue squares in Fig. 1). The blue (red) dots correspond to cases where the skyrmion would be trapped (escape) at $T = 0$. The rest of the parameters are the same as in Fig. 1. The encircled point corresponds to the case of the snapshots in Fig. 1.

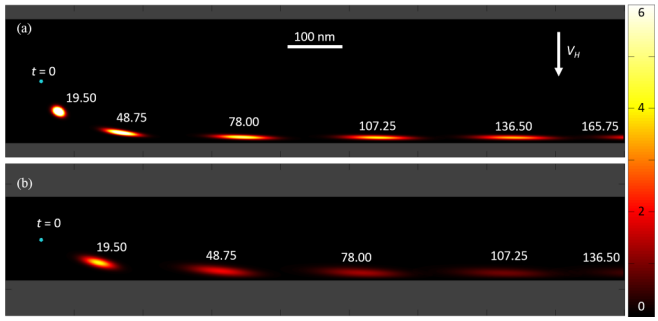

FIG. 3. Snapshots [(a) $T = 100$ K; (b) $T = 300$ K] of the probability density (color bar in units of 10^{-5} nm^{-2}) for the central position of a rigid skyrmion driven along a track, $p(x, y, t)$. In each track, the blue dot (at left) indicates the initial position and $p(x, y, t)$ at several times t (indicated in the figure in ns) are plotted. The gray regions correspond to y's such that $W > |y| > W - \lambda(T)$. The parameters used are $W = 150$ nm, $V_H = 325$ m s^{-1}, $F_{0t} = 5.325 \times 10^{-14}$ m^2 A^{-1}, $\lambda(T = 100\ \text{K}) = 25.05$ nm, $\lambda(T = 300\ \text{K}) = 70.33$ nm. The rest of the parameters are the same as in Fig. 1. See Supplemental Material for numerical details and videos [47].

velocity V_H below the threshold (thus, at $T = 0$, the skyrmion would not escape from the track). When $T > 0$ there is some probability of escaping through the borders due to thermal diffusion.

One interesting figure of merit is the probability that a skyrmion reaches a certain position along the track, which is evaluated from the flux of current density through a section of the track at position x [initially, the skyrmion is located at $(x, y) = (0, 0)$],

$$P_s(x) = \int_{-W+\lambda(T)}^{W-\lambda(T)} dy' \int_0^\infty dt' \, \hat{\mathbf{x}} \cdot \mathbf{J}_p(x, y', t'). \qquad (10)$$

Note that, in order to consider the radius of the skyrmion at different temperatures, apart from considering $\lambda(T)$ in Eq. (9), we have considered that the skyrmion escapes from the track when $|y| > W - \lambda(T)$ (that is, when the "skyrmion border"—not its center—reaches the track border). In Fig. 4(a) we show $P_s(x)$ at different temperatures. The region of $P_s \simeq 1$ corresponds to small distances where the skyrmion has not yet reached the borders. The subsequent decay in the probability indicates that, when the skyrmion is moving along the border, the probability of escaping increases as it goes further away [thus, the $P_s(x)$ track decreases with increasing x].

In Fig. 4(b) we show P_s at a fixed value of $x = x_L$, as a function of temperature, for several values of the driving velocity. In general, the probability of survival up to a given distance decreases with increasing temperature. We observe a plateau, even a slight increase in $P_s(x_L)$ at intermediate temperatures: The confining potential from the borders can compensate the thermal diffusion (and the increase in the radius of the skyrmion) up to a certain temperature and the skyrmion can reach the desired x_L. For large temperatures, the borders are not able to compensate the diffusion and it becomes less likely to reach x_L.

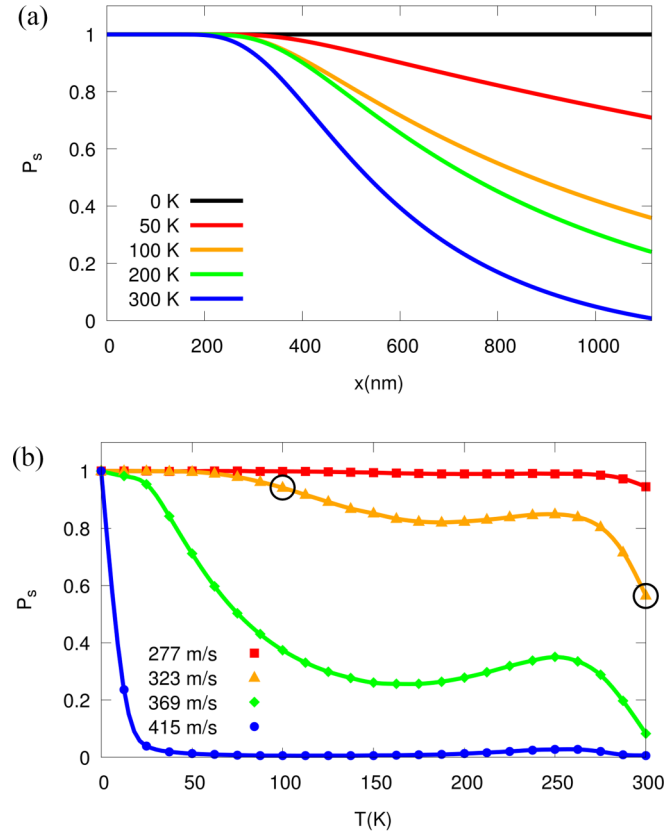

FIG. 4. (a) Probability of surviving a certain distance x along the track as a function of x, $P_s(x)$, for different temperatures (indicated in the figure). (b) $P_s(x_L = 1115\ \text{nm})$ as a function of temperature for different driving currents (indicated in the figure). The parameters not shown are as in Fig. 3. The encircled points in (b) correspond to the simulations of Fig. 3.

Averages over infinite runs of the STE could give the same information as the FPE. Comparing similar computational times and/or precision, the presented calculations are a better approach since the numerical errors in the solution of FPE are orders of magnitude lower that the statistical errors in the averages of the solutions of the STE (see Supplemental Material for a comparison of both methods [47]).

Some of the most promising applications of skyrmions are those based on the one-skyrmion one-bit principle. Knowing the probability of finding a skyrmion at a given position and time is crucial for assessing the viability of such systems at room temperature. Since borders and defects are unavoidable in realistic samples, the present results may help in the future design of skyrmionic devices.

We thank Dr. S. Serna for her advice in the numerical techniques in solving the FPE. We also acknowledge Catalan Project No. 2017-SGR-105 and Spanish Project No. MAT2016-79426-P of Agencia Estatal de Investigación/Fondo Europeo de Desarrollo Regional (UE) for financial support. J.C.-Q. acknowledges a Grant (FPU17/01970) from Ministerio de Ciencia, Innovación y Universidades (Spanish Government).

[1] K. Everschor-Sitte, J. Masell, R. M. Reeve, and M. Kläui, J. Appl. Phys. **124**, 240901 (2018).

[2] A. Fert, V. Cros, and J. Sampaio, Nat. Nanotechnol. **8**, 152 (2013).

[3] G. Bourianoff, D. Pinna, M. Sitte, and K. Everschor-Sitte, AIP Adv. **8**, 055602 (2018).

[4] R. Wiesendanger, Nat. Rev. Mater. **1**, 16044 (2016).

[5] A. Fert, N. Reyren, and V. Cros, Nat. Rev. Mater. **2**, 17031 (2017).

[6] X. Zhang, Y. Zhou, M. Ezawa, G. P. Zhao, and W. Zhao, Sci. Rep. **5**, 11369 (2015).

[7] M. Hervé, B. Dupé, R. Lopes, M. Böttcher, M. D. Martins, T. Balashov, L. Gerhard, J. Sinova, and W. Wulfhekel, Nat. Commun. **9**, 1015 (2018).

[8] S. Heinze, K. von Bergmann, M. Menzel, J. Brede, A. Kubetzka, R. Wiesendanger, G. Bihlmayer, and S. Blügel, Nat. Phys. **7**, 713 (2011).

[9] O. Boulle, J. Vogel, H. Yang, S. Pizzini, D. de Souza Chaves, A. Locatelli, T. O. Mente, A. Sala, L. D. Buda-Prejbeanu, O. Klein *et al.*, Nat. Nanotechnol. **11**, 449 (2016).

[10] A. Sonntag, J. Hermenau, S. Krause, and R. Wiesendanger, Phys. Rev. Lett. **113**, 077202 (2014).

[11] C. Moreau-Luchaire, C. Moutafis, N. Reyren, J. Sampaio, C. A. F. Vaz, N. Van Horne, K. Bouzehouane, K. Garcia, C. Deranlot, P. Warnicke *et al.*, Nat. Nanotechnol. **11**, 444 (2016).

[12] A. Soumyanarayanan, N. Reyren, A. Fert, and C. Panagopoulos, Nature (London) **539**, 509 (2016).

[13] S. Woo, K. Litzius, B. Krüger, M.-Y. Im, L. Caretta, K. Richter, M. Mann, A. Krone, R. M. Reeve, M. Weigand *et al.*, Nat. Mater. **15**, 501 (2016).

[14] J. Sampaio, V. Cros, S. Rohart, A. Thiaville, and A. Fert, Nat. Nanotechnol. **8**, 839 (2013).

[15] T. Schulz, R. Ritz, A. Bauer, M. Halder, M. Wagner, C. Franz, C. Pfleiderer, K. Everschor, M. Garst, and A. Rosch, Nat. Phys. **8**, 301 (2012).

[16] K. Litzius, I. Lemesh, B. Krüger, P. Bassirian, L. Caretta, K. Richter, F. Büttner, K. Sato, O. A. Tretiakov, J. Förster *et al.*, Nat. Phys. **13**, 170 (2016).

[17] A. Salimath, A. Abbout, A. Brataas, and A. Manchon, Phys. Rev. B **99**, 104416 (2019).

[18] V. Raposo, R. F. Luis Martinez, and E. Martinez, AIP Adv. **7**, 056017 (2017).

[19] J.-V. Kim and M.-W. Yoo, Appl. Phys. Lett. **110**, 132404 (2017).

[20] W. Legrand, D. Maccariello, N. Reyren, K. Garcia, C. Moutafis, C. Moreau-Luchaire, S. Collin, K. Bouzehouane, V. Cros, and A. Fert, Nano Lett. **17**, 2703 (2017).

[21] C. Navau, N. Del-Valle, and A. Sanchez, Phys. Rev. B **94**, 184104 (2016).

[22] P. F. Bessarab, G. P. Müller, I. S. Lobanov, F. N. Rybakov, N. S. Kiselev, H. Jónsson, V. M. Uzdin, S. Blügel, L. Bergqvist, and A. Delin, Sci. Rep. **8**, 3433 (2018).

[23] J. Iwasaki, W. Koshibae, and N. Nagaosa, Nano Lett. **14**, 4432 (2014).

[24] J. Castell-Queralt, L. González-Gómez, N. Del-Valle, A. Sanchez, and C. Navau, Nanoscale **11**, 12589 (2019).

[25] J. Miltat, S. Rohart, and A. Thiaville, Phys. Rev. B **97**, 214426 (2018).

[26] R. E. Troncoso and A. S. Núñez, Phys. Rev. B **89**, 224403 (2014).

[27] L. Zhao, Z. Wang, X. Zhang, J. Xia, K. Wu, H.-A. Zhou, Y. Dong, G. Yu, K. L. Wang, X. Liu *et al.*, arXiv:1901.08206.

[28] X. Zhang, M. Ezawa, and Y. Zhou, Phys. Rev. B **94**, 064406 (2016).

[29] L. Desplat, C. Vogler, J.-V. Kim, R. L. Stamps, and D. Suess, Phys. Rev. B **101**, 060403(R) (2020).

[30] S. Rohart, J. Miltat, and A. Thiaville, Phys. Rev. B **93**, 214412 (2016).

[31] R. Tomasello, K. Y. Guslienko, M. Ricci, A. Giordano, J. Barker, M. Carpentieri, O. Chubykalo-Fesenko, and G. Finocchio, Phys. Rev. B **97**, 060402 (2018).

[32] A. Derras-Chouk, E. M. Chudnovsky, and D. A. Garanin, J. Appl. Phys. **126**, 083901 (2019).

[33] J. Müller, New J. Phys. **19**, 025002 (2017).

[34] J. C. Martinez and M. B. A. Jalil, New J. Phys. **18**, 033008 (2016).

[35] U. Atxitia, D. Hinzke, and U. Nowak, J. Phys. D **50**, 033003 (2017).

[36] D. A. Garanin, Phys. Rev. B **55**, 3050 (1997).

[37] J. L. García-Palacios and F. J. Lázaro, Phys. Rev. B **58**, 14937 (1998).

[38] T. Kamppeter, F. G. Mertens, E. Moro, A. Sánchez, and A. R. Bishop, Phys. Rev. B **59**, 11349 (1999).

[39] A. Thiele, Phys. Rev. Lett. **30**, 230 (1973).

[40] T. Nozaki, Y. Jibiki, M. Goto, E. Tamura, T. Nozaki, H. Kubota, A. Fukushima, S. Yuasa, and Y. Suzuki, Appl. Phys. Lett. **114**, 012402 (2019).

[41] J. Zázvorka, F. Jakobs, D. Heinze, N. Keil, S. Kromin, S. Jaiswal, K. Litzius, G. Jakob, P. Virnau, D. Pinna *et al.*, Nat. Nanotechnol. **14**, 658 (2019).

[42] H. Risken, *The Fokker-Planck Equation* (Springer, Berlin, 1984).

[43] R. Khoshlahni, A. Qaiumzadeh, A. Bergman, and A. Brataas, Phys. Rev. B **99**, 054423 (2019).

[44] A. V. Bondarenko, E. Holmgren, B. C. Koop, T. Descamps, B. A. Ivanov, and V. Korenivski, AIP Adv. **7**, 056007 (2017).

[45] L. Liu, O. J. Lee, T. J. Gudmundsen, D. C. Ralph, and R. A. Buhrman, Phys. Rev. Lett. **109**, 096602 (2012).

[46] L. González-Gómez, J. Castell-Queralt, N. Del-Valle, A. Sanchez, and C. Navau, Phys. Rev. B **100**, 054440 (2019).

[47] See Supplemental Material at http://link.aps.org/supplemental/10.1103/PhysRevB.101.140404 for the derivation of the FPE equation for rigid skyrmions, details for the model and the numerical solution, comparison between STE and FPE performance, and videos of the simulations.

[48] W. Jiang, X. Zhang, G. Yu, W. Zhang, X. Wang, M. B. Jungfleisch, J. E. Pearson, X. Cheng, O. Heinonen, K. L. Wang *et al.*, Nat. Phys. **13**, 162 (2016).

[49] A. Kurganov and E. Tadmor, J. Comput. Phys. **160**, 241 (2000).

[50] J. Müller and A. Rosch, Phys. Rev. B **91**, 054410 (2015).